7

The effects of corrosion and fouling on the performance of ocean-going vessels: a naval architectural perspective

T MUNK and D KANE, Propulsion Dynamics Inc., USA and
D M YEBRA, Pinturas Hempel S.A., Spain

Abstract: The primary role of antifouling precautions on ship hulls is to avoid the tremendous increase in drag resistance caused by the settlement of fouling species. In this chapter, basic hydrodynamic concepts needed to fully understand the effect of fouling species on the propulsion requirements of a ship will be introduced. Subsequently, studies on the drag resistance associated with various coating types and fouling species are reviewed. Finally, the main topic of this chapter is to discuss how to monitor the hydrodynamic performance of an antifouling coating applied to an actual ship during service through appropriate data logging and mathematical models.

Key words: drag resistance, boundary layer, hull roughness, hydrodynamics, ship powering.

7.1 Ship hydrodynamics basics

The primary role of a ship antifouling coating is to limit the increase in frictional drag as a result of surface deterioration and biofouling accumulation. Frictional drag alone can account for as much as 90% of the total drag on some hull types, even when the hull is relatively smooth and unfouled (Schultz, 2007). Hence, for a given ship design, the coating condition is crucial to the performance of ships. Frictional drag in a ship is directly linked to the interaction between the moving hull and the surrounding seawater. As the ship moves, a significant mass of water, sometimes reaching 1/4 or even 1/3 of the total mass of the ship, is accelerated to a speed close to that of the ship. The consequence of this is that the engine must deliver additional power to keep constant speed.

The boundary layer is the area closest to the hull in which the fluid is impeded as a result of its viscosity. The relative velocity at the surface of an object is zero (no-slip condition) and, at some distance away from the object, the velocity is the freestream value. In the layer between the two, there must be a velocity gradient. The thickness of the boundary layer, δ, increases down the length of the hull and may reach a meter or more in thickness on a large ship (Schultz and Swain, 2000). In a boundary layer developing over a surface, the flow remains laminar for a distance downstream. After some development, instabilities arise, and the flow begins to transition to turbulence. The transition for the case of a smooth flat plate occurs approximately when:

$$\mathrm{Re}_x = \frac{U_e \cdot x}{\nu} > 1 \cdot 10^6 \qquad 7.1$$

Re_x is the Reynolds number at point x placed x meters downstream.
U_e is the freestream fluid velocity and ν is the kinematic viscosity of the fluid.

For a ship moving at 10 m/s (almost 20 knots), transition takes place at about 10 cm downstream of the bow. We will therefore focus on turbulent boundary layers, which cover the majority of the hull. Further downstream, the boundary layer may detach from the hull, and flow reversal may occur (point of separation).

Ship powering requirements are directly linked to the shear stress along this boundary layer. In the boundary layer, the total shear stress is made up of both viscous ('laminar') and Reynolds ('turbulent') stresses.

$$\tau = \mu \cdot \left(\frac{\partial U}{\partial y} \right) - \rho \cdot \overline{u'v'} \qquad 7.2$$

To understand the meaning of viscous drag, one needs to imagine the fluid as layers move smoothly over each other without macroscopic mixing. The layers close to the hull have higher velocity and therefore there is a shear stress between these and the upper layers further away from the hull surface. In turbulent flow the particles move both horizontally and vertically and there is a continuous 'mixing of particles' causing continuous exchange of momentum.

Figure 7.1 shows a typical shear stress profile as a function of the normalized distance from the wall (y^+).

Wall roughness, in the form of, e.g. fouling or coating defects, leads to increased turbulence and fluid mixing in the boundary layer. This manifests itself as increased turbulent and wall shear stress (i.e., increased powering requirements). Before discussing the effect of fouling on ship drag, we will introduce some basic boundary layer concepts.

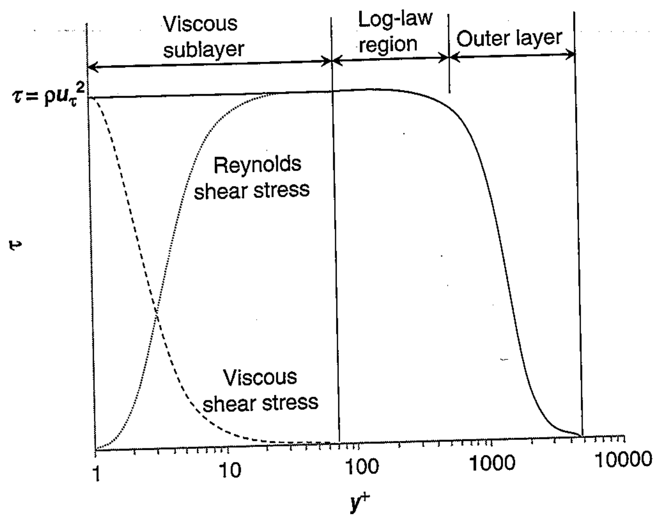

7.1 Turbulent boundary shear stress profile as a function of dimensionless distance from the hull. Adapted from (Schultz and Swain, 2000). 'y^+' equals $y \cdot U_\tau \cdot \nu^{-1}$. U_τ is the friction velocity and equals $(\tau_w/\rho)^{1/2}$, with τ_w being the wall shear stress and ρ the seawater density. ν is kinematic viscosity of the fluid and y is the distance from the hull.

7.2 Turbulent boundary layer basics

The turbulent boundary layer is considered to consist of several regions characterized by their water velocity profile. These regions include the viscous sublayer, the log-law region, and the outer region (Fig. 7.2).

1. The viscous sublayer covers the innermost 10–20% of the turbulent boundary layer $y/\delta = 0.1$–0.2. Despite its low thickness, about 70% of the velocity gradient is found in this region. The local mean velocity in this region is a function of the wall shear stress, fluid density, kinematic viscosity, and distance from the wall. The law of the wall is expressed as:

$$\frac{U}{U_\tau} = f\left[\frac{y \cdot U_\tau}{\nu}\right] \Rightarrow U^+ = f[y^+] \qquad 7.3$$

U_τ is the friction velocity and is expressed as the square root of the ratio between the wall shear stress τ_w and the fluid density.

$$U_\tau = \sqrt{\frac{\tau_w}{\rho}} \text{ with } \tau_w = \mu \cdot \left(\frac{\partial U}{\partial y}\right)_{y=0} \qquad 7.4$$

The viscous sublayer consists of two parts, the linear sublayer and the buffer layer.

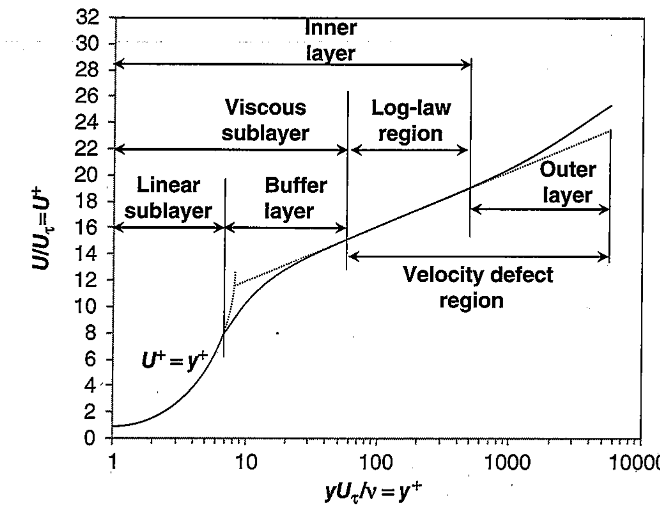

7.2 Law of the wall plot for a turbulent boundary layer (from Schultz and Swain, 2000).

i. Linear sublayer: $y^+ \leq 7$, $U^+ = y^+$. Across this layer the total shear stress is almost constant and equal to the wall shear stress (Fig. 7.1). The wall shear stress is often normalized with the dynamic pressure to form the skin friction coefficient:

$$C_f = \frac{\tau_w}{1/2 \cdot \rho \cdot U_e^2} \qquad 7.5$$

where U_e is the mean axial velocity at the edge of the boundary layer.

ii. Buffer layer: $7 < y^+ < 40$. The velocity profile departs from linearity and shows high turbulence.

2. Log-law region: the flow just outside the viscous sublayer ($y^+ > 40$) and with $y/\delta > 0.15$ is also highly turbulent in nature. In this region, also called the log-law region, we find that:

$$U^+ = A \cdot \log(y^+) + B \qquad 7.6$$

3. Outer region: in this layer the difference between the freestream velocity and the local mean velocity U at a distance y from the wall is determined by the boundary layer thickness δ and the friction velocity U_τ.

$$\frac{U_e - U}{U_\tau} = g \cdot \left(\frac{y}{\delta}\right) \qquad 7.7$$

where $g(y/\delta)$ is a universal function (Schetz, 1993)

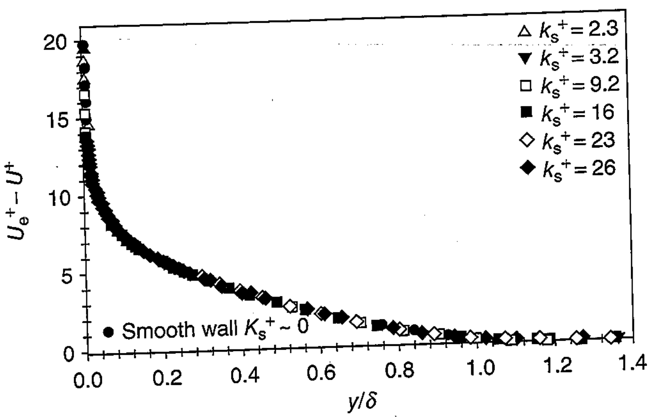

7.3 The velocity profiles in the outer layer are shown to be largely insensitive to the surface roughness (Schultz, 2007). Reproduced with permission from Taylor & Francis.

This region is thought to be independent of surface roughness, except for its influence on setting the velocity (U_τ) and length (δ) scales. Figure 7.3 depicts the turbulent boundary layer mean velocity profiles throughout the boundary layer showing the insensitivity of the outer layer to the surface roughness. In this plot, the roughness height, k, is assumed to be equal to the equivalent sand roughness height, k_s, for the case of uniform, tightly packed sand, which gives the same roughness function as the roughness of interest in the fully rough flow regime (Schultz, 2007).

7.2.1 Wall roughness

Wall roughness leads to increased turbulence and fluid mixing in the boundary layer. This phenomenon manifests itself as increased turbulent and wall shear stress. For most surfaces the increased skin friction depends somehow on 'k,' the roughness height. Three distinct flow regimes can be identified for this type of roughness depending on the value of the roughness Reynolds number:

$$k^+ = \frac{k \cdot u_\tau}{\nu} \tag{7.8}$$

1. Hydrodynamically smooth regime: $k^+ < 5$ (or 3, according to Schultz and Flack, 2007) and the roughness elements are sufficiently small to be completely submerged in the linear sublayer. In this case, the skin friction is equal to a smooth surface and is dominated by the viscous component.
2. Intermediate regime: $5 < k^+ < 70$ (25, according to Schultz and Flack's tests), the skin friction is increased, and τ_w depends on both viscous and turbulent components. This is the most significant for the majority of practical full-ship conditions.
3. Fully rough regime: $k^+ > 70$, the linear sublayer is completely destroyed, and τ_w is dominated by the turbulent components.

If we look at the velocity profile within the boundary layer, the effect of roughness can be expressed as:

$$U^+ = \frac{1}{\kappa} \cdot \log(y^+) + B - \Delta U^+ \tag{7.9}$$

where κ is the von Karman constant (= 0.41), B is the smooth wall log-law intercept (= 5), and ΔU^+ is the roughness function.

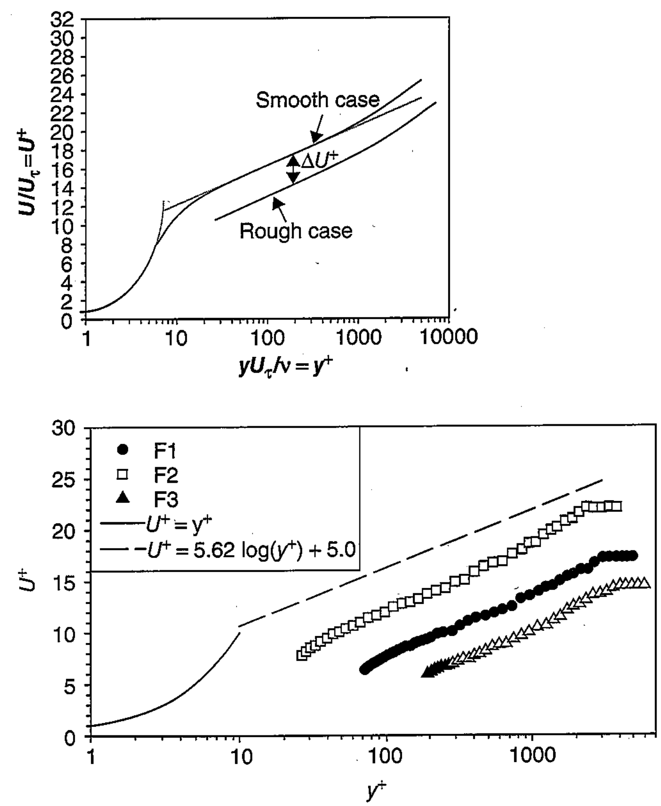

7.4 The theoretical effect of roughness on the law of the wall (top). On the bottom, experimental measurements showing the effect of biofilms on the law of the wall as measured by Schultz and Swain (2000) are shown. Reproduced with permission from Taylor & Francis.

ΔU^+ expresses a downward shift of the velocity profile of the log-law region and is directly related to the increase in frictional drag of the surface (momentum deficit). Unfortunately, a general correlation between ΔU^+ and measurable surface parameters (represented as k^+) does not exist, despite several attempts to find one are reported in the literature (Schultz and Swain, 2000). The relationship between different fouling types and roughness is elaborated further in Section 7.4.

An example of the effect of increased roughness (slime buildup, in this case) on the velocity gradient across the boundary layer is shown in Fig. 7.4 (Schultz and Swain, 2000).

7.3 Coating type and associated drag

Soon after the introduction of foul release coatings in the mid 1990s, it became evident that the choice of coating type does influence a ship's hull resistance right after application. Long-term fouling deterrence is the most important feature when discussing the drag performance of an antifouling coating, as stated by Weinell *et al.* (2003) (Fig. 7.5). In other words, any initial positive influence that coatings have on ship drag are meaningless unless such effects can be maintained during immersion time until the next dry-

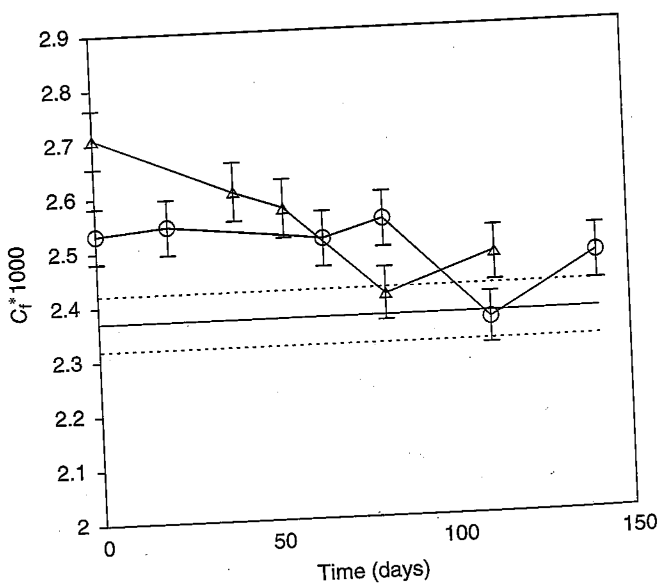

7.5 Decrease in the friction coefficient with dynamic exposure time as a result of self-smoothing of the topcoat. From Weinell *et al.* (2003). Reproduced with permission from Taylor & Francis.

docking operation (as much as 60 months later in many cases). In spite of this, a number of tests have been carried out in the last few years comparing the drag resistance of freshly applied fouling-free silicon coatings to that of traditional self-polishing paints in fouling-free waters (Table 7.1). In all studies, silicone topcoats demonstrate improved hydrodynamic behavior compared to eroding-type paints. This difference is hypothesized to result from differences in surface texture, as reported in Candries *et al.* (2003). While tin-free SP coatings presented a spiky 'closed' texture, the silicon topcoat featured a wavy 'open' texture with a smaller proportion of short-wavelength roughness (Anderson *et al.*, 2003). On top of this, current fouling release coatings are usually applied after a full blasting of the hull, which is also expected to smooth out hull roughess inherent to old hulls hence providing additional fuel savings (see, e.g., Section 7.10). Only the study by Holm *et al.* (2004) reports higher drag resistance for a silicone topcoat compared to an eroding-type coating, but those measurements were performed after cleaning the fouling settled on the different topcoats after three weeks of static exposure in Chesapeake Bay. Hence, small-scale surface damage may be responsible for such results.

In Table 7.1, it is also important to note that self-polishing topcoats do smooth out during service, as demonstrated by Weinell *et al.* (2003), which is not reflected in the above studies. To the author's knowledge, there exists no systematic study comparing drag behavior of fouling control coating families with ageing time in the presence of fouling species under realistic speed-activity conditions. Schultz (2004), as an example, compares self-polishing and fouling relase topcoats after static exposure to natural seawater, which are not the most relevant conditions for fouling release topcoats.

Table 7.1 Representative differences in friction coefficient when comparing clean fouling release coatings to self-polishing type ones. Non-fouled silicone topcoats are reported to consistently decrease the drag resistance of a hull compared to eroding-type paints

Source	ΔC_F%	Remarks
Weinell *et al.* (2003)	6.1%	Rotary study. Topcoat on smooth PVC
Candries *et al.* (2003)	3.5%	Rotary study. Full system on smooth PVC
Schultz (2004)	3.0–3.8%	Full system on 304SS. No sandpaper strip
Holm *et al.* (2004)	–2.5%	Friction disk machine. After biofilm removal. Potential surface damage
Candries and Atlar (2005)	5.3%	Topcoat on smooth steel. Turbulent boundary layer measurements
Anon (2008)	1.4%	Towing test. Full system on smooth Al/smooth undercoats

7.4 Fouling species and related drag

As mentioned before, it would be quite convenient to be able to relate ΔU^+ (i.e. indirectly C_f) to measurable surface parameters (represented as k^+). Ideally, such a correlation would also be applicable to fouling species, so that we could estimate increased hull resistance for almost any hull condition. Unfortunately, the latter is quite a difficult task, especially given the enormous complexity and variability of fouling communities.

Townsin (2003) provided a summary of reported drag increase associated with different fouling species from real-life ship measurements (Table 7.2). It is important to note that this type of measurement has a very high associated uncertainty, as discussed in the second part of this chapter.

Schultz and Swain (2000) carried out laser Doppler velocimeter (LDV) boundary layer measurements on heavily slimed specimens in a water channel. Large scattering in the increased C_f as a result of the growth of biofilms on the acrylic panels was reported, with values reaching 370% in specific cases. Holm *et al.* (2004) reported a drag increase of 9–29% from friction disk machine measurements of slimed, fouled topcoats. The disks had been exposed under static conditions for three weeks in Chesapeake Bay. Schultz (2004) carried out towing tank tests with panels immersed for more than nine months at Severn River (Annapolis). For the silicone plates (worst case), the C_f increased 300–400%, while 4% barnacle fouling on an ablative copper coating increased the C_f by 138%. In the same study, a thin slime film on a tributyltin self-polishing copolymer paint was reported to increase drag by 58–68%.

Perhaps the best summary of all of the above information comes from the attempt by Schultz (2007) to relate the hull fouling condition to equivalent sand roughness height k_s and the average coating roughness (Rt_{50}; Table 7.3).

Naval Ships' Technical Manual (NSTM) ratings below 30 are used to denote coverage of soft fouling only. A rating of 40 indicates the initial

Table 7.2 Reported effect of fouling on the hull's frictional resistance (see Townsin, 2003 and Schultz and Swain, 1999 for full reference list)

Slime	5%	Conn *et al.* (1953)
	8–14%	Watanabe *et al.* (1969)
	18%	Lewkowicz and Das (1986)
	10–20%	Loeb *et al.* (1984)
	25%*	Lewthwaite *et al.* (1985)
	8–18%*	Bohlander (1991)
Shell and Weed	85%	Kempf (1937) 75% coverage shell 4.5 mm.

* Also some hard fouling and/or macroalgae.

Table 7.3 Reported effect of different hull conditions on the total resistance and shaft power for the case of US Navy Oliver Hazard Perry class frigate. Increased fouling severity, represented as increased average coating roughness (Rt_{50}) and equivalent sand roughness height (k_s) values, involves higher frictional resistance and, consequently, higher powering demands to keep a speed of 15 knots (Schultz, 2007).

Description of condition	NSTM rating	k_s (μm)	Rt_{50} (μm)	ΔR_t (%)	ΔSP (%)
Hydraulically smooth surface	0	0	0	–	–
Typical as applied AF coating	0	30	150	2	2
Deteriorated coating or light slime	10–20	100	300	11	11
Heavy slime	30	300	600	20	21
Small calcareous fouling or weed	40–60	1000	1000	34	35
Medium calcareous fouling	70–80	3000	3000	52	54
Heavy calcareous fouling	90–100	10000	10000	80	86

presence of calcareous fouling. As the degree of shell fouling increases, the rating rises to a value of 100, which is given for heavy, large-size shell fouling. The increase in C_f as a result of increased surface roughness is estimated using the similarity law scaling procedure for the case of the US Navy Oliver Hazard Perry class frigate. This frigate has a waterline length of 124.4 m with a beam of 14.3 and displaces 3779 tonnes. Different results would be obtained for larger trading ships such as tankers and container vessels. The increased total resistance and shaft power for the above-mentioned ship sailing at 15 knots are given in Table 7.3.

7.5 Introduction: fouling and ship powering

Marine biofouling begins to accumulate on the submerged portion of an oceangoing vessel within minutes of making contact with the water. Over time, this accumulation increases the drag of the vessel, causing the physical resistance of the vessel to increase. As a result of fouling drag on the vessel, higher fuel consumption to maintain a given speed or lower speeds at a maintained power will occur.

Owners of oceangoing vessels spend considerable time and money to mitigate the effects of fouling on vessel performance. Mitigation can be accomplished by several means, including pre-treating the surface of the hull in drydock, as well as increasing the frequency of vessel drydocking, which usually takes place every 2½ to 3 years or 5 years, depending on the age of the vessel. In addition, a wide variety of coating manufacturers and antifouling technologies are available, depending on vessel type, speed, trading area, activity rate (time away from ports), and geographic voyage pattern.

Typical costs of hull treatment during a drydocking can range from tens of thousands of dollars to several million dollars depending on vessel size, the type of coating system applied, and the pretreatment of the hull prior to the coating application. Between drydockings, the vessel operator may undertake hull cleanings or propeller polishing in order to regain some of the vessel performance losses resulting from fouling and corrosion. Hull cleanings cost between 10 000 and 30 000 USD depending on the portion of the underwater hull that is cleaned and the cleaning technique employed, and may require between one and three days in port. Propeller polishing costs range from 2000 to 5000 USD and can be done in one day.

TBT coatings were developed in the 1970s, and over a period of 20 years have proven to exhibit an excellent ability to prevent fouling accumulation, including slime (mainly bacterial; see Chapter 17 for more details.) The ban on TBT coatings enacted by the International Maritime Organization in 2003 spurred the development of many new coating systems. These modern alternatives contain less toxic biocides; however, as a result of the presence of less effective – or, in some cases, no – biocides in the coating, the rate of fouling on vessel hulls is in general higher than with the good-quality TBT predecessors. Over the period of a three- or five-year drydocking interval, the advantages of efficient pretreatment and good-quality coating systems become more important, given higher fuel costs and governmental interests in mitigating the biorisk associated with heavily fouled hulls.

The interest in sustaining high hull and propeller efficiency in the total picture of economic and environmental efficiencies has increased substantially over the past few years, mainly due to higher fuel prices, as well as pressures to reduce marine vessel emissions and mitigate the translocation of marine biofouling pests attached to the underwater portion of vessel hulls. The following section will examine in more detail vessel performance and the effect of fouling on the speed–power relationship for typical oceangoing vessels with single displacement hulls.

It should be kept in mind that the overall CO_2 and GHG emissions from oceangoing vessels are extremely low (emissions per ton-mile of goods moved) within the context of all modes of transportation (Swedish Network for Transport and the Environment). Nevertheless, more efficient, non-toxic antifoulant systems for the underwater portion of the hull will still benefit the environment greatly.

7.6 Background on vessel performance

Many vessel owners are not aware of the true impact that fouling has on vessel performance, owing to the inherent limitations of performance monitoring systems. Nowadays, methods for more precise analysis of vessel performance, based on the standard measuring equipment onboard, are

available, as will be described in this chapter together with some examples of the results that have been achieved.

7.6.1 How vessel performance is measured

For most vessels delivered from a shipyard there is a diagram showing the relation between speed and required power for one or more loading conditions, as shown in Fig. 7.6. This diagram has been prepared based on theoretical calculations and in most cases has been confirmed by towing tank tests. The towing tank is a basin, several meters wide and hundreds of meters long, equipped with a towing carriage that runs on two rails. The towing carriage can either tow the model or follow the self-propelled model, and is equipped with computers and devices to register or control, respectively, variables such as speed, propeller thrust and torque, rudder angle, and so on. The towing tank serves, in resistance and propulsion tests with towed and self-propelled ship models, to determine how much power the engine will have to provide to achieve the speed laid down in the contract between shipyard and ship owner. Figure 7.6 is an example of the power versus speed diagram derived from the towing tank and/or from sea trials.

7.6.2 Sea trials

Formal speed trials are a necessary procedure for fulfilling contract terms between the shipyard and ship owner. Contract terms usually require that the speed be achieved under specified conditions of draft and deadweight, a requirement met by runs made over a measured ocean course. This speed trial is a complicated and time-consuming procedure. The vessel must be loaded correctly, the weather must be reasonably good, and the trial must take place in a test area with deep water at a time when there is no other

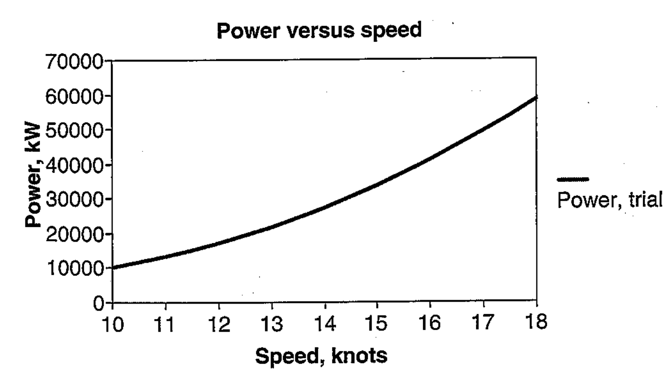

7.6 Theoretical power versus speed for an oceangoing vessel.

immediate traffic. Time must be given to accelerate the vessel up to a constant steady-speed and, as a sea current may be present, each speed run has to be made twice in opposite directions to compensate for this. Consequently, only a limited number of draft/speed combinations are tested, so the achieved speed/power results, properly adjusted for wind, waves, temperature, salinity, and draft differences, are used merely to confirm or adjust the already existing diagram.

7.6.3 Sea trials: power versus speed

If the engine's maximum continuous rating (MCR) is plotted in this diagram, the maximum speed for the ship may be found, as illustrated in Fig. 7.7.

Vessel owners know that this is not the speed they can expect in daily operation; for commercial consideration, they define a so-called 'service speed.'

7.6.4 Vessels in service: power versus speed

This service speed is traditionally found by adding 15% to the power curve and subtracting 15% from the engine power line, as shown in Fig. 7.8. The 15% added power is expected to consist of 5% for weather losses and 10% for losses due to hull and propeller surface roughness caused by marine growth and corrosion. For a well-organized introduction to ship propulsion, see Man (2004).

The actual situation with respect to marine fouling for any particular vessel may be worse. This situation will only be discovered if the fouling is significant, because it is very difficult in practice to obtain a reliable and accurate picture of the speed/power performance of a vessel in service.

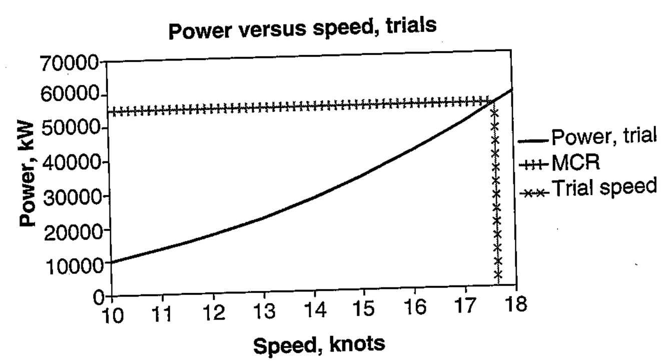

7.7 Actual power versus speed for an oceangoing vessel confirmed by sea trials.

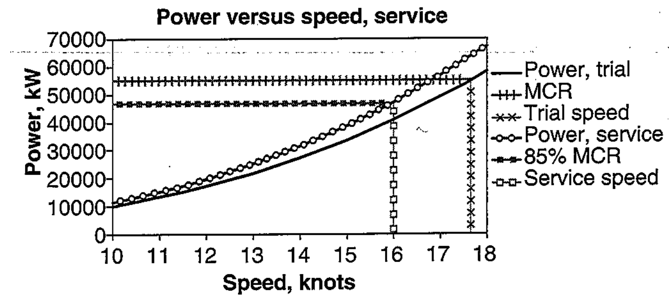

7.8 Service speed calculation for an oceangoing vessel.

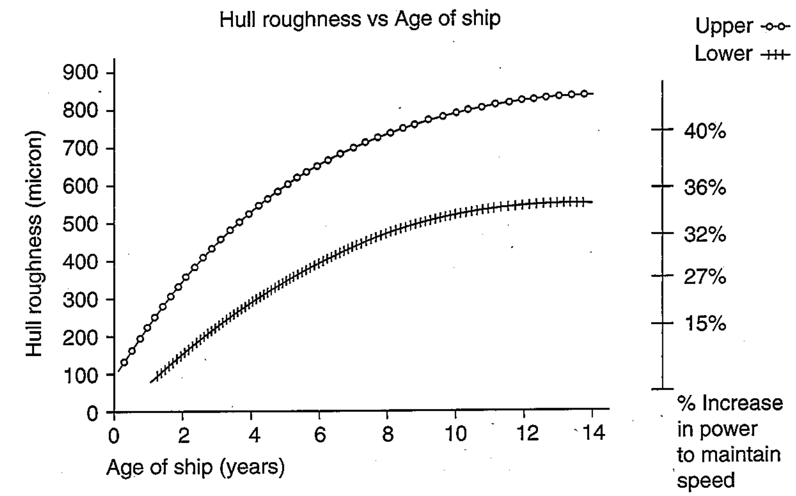

7.9 Increased average hull roughness with ship age and effect on powering.

Estimates of increases in fuel consumption from biofilm attached to the hull alone range from 8% to 12%, and from normal propeller fouling range from 6% to 14% (Haslbeck, 2003). Hull and propeller fouling are the topic of increased focus as causes of increased fuel consumption and corresponding increases in GHG emissions from oceangoing vessels (Buhaug, 2005).

7.7 Degradation of vessel performance

The main reason for performance degradation is marine growth and roughness on the vessel's hull. Figure 7.9 shows the hull roughness increasing over time and the increased power needed to maintain speed (or speed losses at a maintained power; Swain, 2007). This is because the ship's viscous resistance increases markedly with increasing roughness (IMO, 2000). More careful hull pre-treatment and coating application work during drydock stopovers (at 5, 10 and 15 years) would halt or reduce this hull roughness increase.

Vessel managers devote resources of time and money to prevent or mitigate the degradation. The main remedies are various types of hull surface preparation in drydock, coatings applied to the underwater portion of the hull at regular intervals (see, e.g., Chapter 18), and in some cases, in-water cleaning of the hull and/or polishing of the propeller. Many factors are emerging in the shipping industry that make the investigation of hull fouling as a mode of invasive species translocation more important. These factors include larger vessels that travel farther and faster, as well as the ban on TBT hull-coating systems, considered the most successful antifouling coatings ever developed (Swain, 2007).

Altogether, the total costs of all vessel owners' antifouling precautions are of the order of 1.5 billion USD per year, or approximately 5% of total marine fuel oil costs. Unfortunately, it is difficult for an owner/operator to determine whether this money is optimally invested. There are many different types of hull treatments, and the price for the coatings varies greatly. In addition, each vessel owner has his or her own way of handling coating selection and directing efforts to control marine fouling. Furthermore, it is difficult to evaluate and compare the effect of the different hull treatments, unless reliable methods of performance analysis are available.

7.7.1 Monitoring of vessel performance

Most vessel operators have established a procedure for speed/power monitoring, for instance by measuring the daily fuel consumption and the daily distance covered at noon-time when nice weather prevails. In this way, the daily mean power and mean speed may be calculated, and the result may be plotted in the speed/power diagram for comparison with the trial trip results. Unfortunately, results achieved in this way usually scatter so much that it is impossible to conclude anything directly from such a diagram, as may be seen from Fig. 7.10, which is a plot for a well-maintained containership.

Procedures may also have been established for more precise measurements at longer intervals – for instance, once a month. A day with good weather may then be chosen. In such cases, and where the prime mover is a slow-running diesel engine, the power may be measured more accurately by cylinder indication, and speed may be measured over a period of time (for instance, two hours) at constant power on a constant course. The result of such an exercise will be more accurate than one based on 'noon data;' however, even such monthly results scatter to an extent that an accurate service speed prediction may be difficult or impossible to obtain.

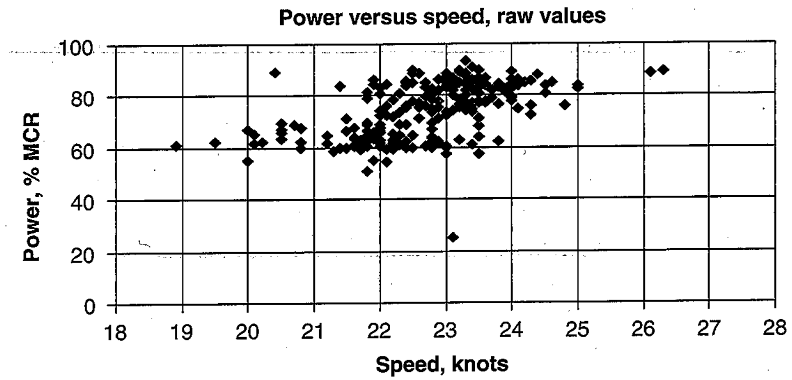

7.10 Power versus speed: raw performance data for an oceangoing vessel.

Underwater inspections of the hull as a supplement to speed and power measurements are of course useful; however, they do not provide a meaningful metric between fouling and impact on vessel performance.

7.7.2 Factors influencing speed/power monitoring

There are many reasons why the directly obtained speed/power values are scattered as in the above illustration. The main factors that need to be taken into account are:

1. Drafts. Mean draft and trim has a great influence on the vessel resistance. It is reasonably easy to adjust the results for differences in mean draft, but differences in trim are more difficult to deal with, especially when most ships today are equipped with a bulbous bow.
2. Weather. Wind and waves can seldom be ignored; therefore, the results will need to be corrected accordingly. It is not that difficult to measure and make corrections for the wind, but waves can neither be measured (by instruments) nor be easily corrected for.
3. Sea current. Today the speed over ground may be measured with great accuracy by means of the DGPS; however, this speed will not be the true speed due to the presence of sea current. The true speed, the speed through the water, is more difficult to measure. The problem is that there is no assurance that the speed-log is measuring speed outside of the ships boundary layer. Normally, it will not be possible to correct the speed for sea current unless a reciprocal run is performed, and this extra step is too time-consuming to be done during commercial operation.

4. Temperature and salinity. These two factors do have some influence on analysis results, but are seldom taken into account in performance analysis by vessel owners/operators.
5. Last but most importantly: the lack of a method for interpreting results. Even if reliable speed/power values, corrected for all the above-mentioned factors, are obtained and plotted in the speed trial speed/power diagram, it may be difficult accurately to describe the degradation of the performance, because the ship's resistance may be roughly divided into frictional resistance and wave-making resistance. Fouling only influences the frictional resistance, and as the frictional resistance fraction of the total resistance depends on the speed and the draft, the additional power demand, expressed as percentage of the total power requirement, will not be the same for different loading conditions and different speeds.

Note: other causes of changes in resistance of a vessel involve loss in efficiency of the engine; however, engine/bearings/propeller shaft degradation will not manifest itself in the same way as hull or propeller fouling, but in other ways – for example, as a high-exhaust gas temperature of one or more cylinders.

7.8 Methods for measuring vessel performance losses due to fouling and corrosion

The effect of hull resistance on propulsion performance is complicated to describe in an unambiguous way. The primary effect is that more water is dragged forward along with the vessel, and this phenomenon will of course increase the vessel resistance. The increased forward velocity of the water in the vessel's boundary layer will also cause the inflow velocity to the propeller to be reduced. This reduced inflow has several effects. On one hand, the efficiency of the propeller will decrease; on the other hand, some of the power lost in the boundary layer will be regained. Altogether, the required power will increase, though not quite as much as the resistance. Since it is not possible to state a fixed relation between added resistance and added power, for simplicity it is proposed to use the 'added resistance' as a measure for degradation and *not* the added power. A vessel's added resistance may be helpful in establishing a CO_2 Operational Index for oceangoing vessels, since specific ship resistance affects fuel consumption (Delft, 2006).

Even describing hull degradation in the form of the added resistance as a percentage of the total resistance is ambiguous, unless it is specifically designated for which speed and which loading condition (draft) this percentage is valid. Therefore, it is further proposed to refer the added resistance to 'the design speed and the design draft.' This is not a precise reference, but it works in practice and is quite useful not only for evaluating the condition of a single vessel, but also for comparing several vessels, which do not need to be of the same shape and size. At deep draft and low speed the power increase will be more than the added resistance, and in ballast condition at full speed it may be less than half of the added resistance (Schultz, 2007). Note that it is always possible to calculate the actual power increase for any draft/speed from the found added resistance. The implication here is that the fouling factor for different coating systems may be compared, even if they are applied to vessels of different size or hull form.

7.8.1 Collection of performance data

As mentioned above, performance data may be collected daily or, in a more detailed form, at an interval of a month or so. Some vessels have an automatic data logging system that files performance observations continuously.

In principle, any of these methods may be relevant and useful, as long as the observations are made carefully. These different methods do have their advantages and disadvantages:

1. Continuous data logging excludes all human errors, but some data, for instance wave data, are normally not available in this way. Furthermore, this method produces a lot of data, which means that some kind of data reduction or data selection needs to be introduced together with the system. Even if wave data are recorded in some automatic fashion, it remains difficult to assure that only data for valid navigation conditions are further processed.
2. Daily performance observations, the so-called 'noon-data,' are useful for some purposes if carefully dealt with. Daily reports can only be used for reliable performance analysis if all conditions have remained unchanged during the 24-hour noon-to-noon period, but this is seldom the case.
3. Monthly, detailed observations over a time interval of a couple of hours are normally as reliable as such observations can be and quite useful. It will be described later that these observations cannot stand alone, but need to be treated together. Twelve sets of performance observations a year are therefore too few to establish a reliable 'time history' for the development of the added resistance for a ship.
4. A reasonable solution seems to be a procedure in which observations are made once a week. This interval is so short that the routines are not forgotten, but on the other hand is long enough that careful attention can be placed on this new dataset. In addition, it is usually possible to find a two-hour period with constant navigation conditions within a time interval of a week, and ±50 observations per year is adequate for a detailed time history of the propulsion efficiency.

7.8.2 Processing of performance data

One way of processing the performance data is to compare the observed power and RPM values to those found for similar weather and loading conditions from a mathematical model of the vessel's propulsion performance. It can then be determined at which speed through the water and with which added resistance the calculated values match the measured values, and both speed through water and added resistance are then determined.

This method requires that such a mathematical model be available or be possible to establish, but creating such a model is not as easy as it sounds (Townsin, 2003) There are complicated theoretical methods for the calculation of resistance, propulsion system performance, weather resistance, and influence of hull resistance for a specific vessel, but in practice a robust general mathematical model that can easily be adapted to any vessel is needed. Such a model may be established by means of a combination of theoretical considerations and approximation formulas with empirical constants.

The number of empirical constants in a model developed in this way is quite high, but fortunately, some of these values are valid for all vessels or for large groups of similar vessels. Other constants are specific to individual vessels. The value of some of these latter constants may be found by careful analysis of the tank test and/or trial trip results, whereas other constants can only be found by statistical analysis of a sufficient number of performance observations for the vessel in service.

As an example, CASPER® is based on a general mathematic model; it is a build up by well-known, state-of the art elements for the calculation of vessel resistance, propeller performance, weather resistance, and so on. The general model, based on the type and main dimensions of vessel and propeller, may stand alone and may be used directly for comparison to actual performance data, but a more reliable model can easily be established by adjusting the general model, considering tank test/trial data. Even this model will not normally reflect all changes in the operational conditions, and the model is therefore not used for performance evaluation until it has been adjusted further by means of a statistical analysis of a number of performance observations. In general, 10–12 sets of performance observations are required (in some cases, the standard noon reports can be utilized) for this purpose, and the model will then be used for performance analysis and predicting speed/fuel penalties due to fouling. The adjustment of the model continues weekly, as more observation data are received. Normally, the basic constants of the model will remain unchanged after 30–40 sets of observations, but the constants describing the condition of the hull and propeller resistance are updated in real time as service performance data from the vessel is acquired.

7.8.3 Accuracy of the analysis

In practice, the accuracy of the analysis results depends more on the accuracy of the performance observation data than of the mathematical model itself. Experience shows that the actual added resistance as earlier described may be found with an accuracy of approximately 1%, and that the result from a single set of observations normally will not deviate more than 3% from the mean value. The actual speed/power diagrams that may be produced from the adjusted mathematical model are therefore fully valid for all practical purposes (transport cost calculations, cost-benefit decisions for coating selection, optimal maintenance intervals, etc.).

7.9 Added resistance diagrams and their use

In the following, an added resistance diagram is shown for three vessel types in order to illustrate the described method. The individual analysis results are shown, and a first-order curve (a straight line) is faired through the points in order to show the development. For each vessel, there is a direct relationship between added resistance (fouling factor) and speed/fuel penalties.

7.9.1 Tankers

1. A typical example (see Fig. 7.11) of development of added resistance. It is seen that the added resistance of the hull and propeller in this case develops very slowly, less than 0.5% per month.

7.9.2 Containerships

2. An example (see Figs 7.12, 7.13 and 7.14) of a more pronounced development of added resistance. At 24 knots, the propeller polishing at

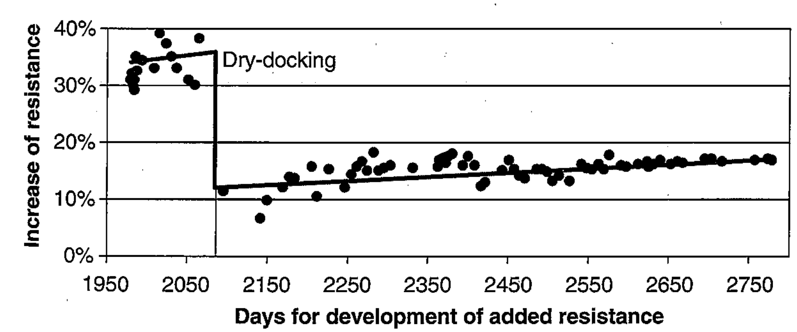

7.11 Added resistance diagram illustrating the decrease in resistance due to drydocking hull treatment.

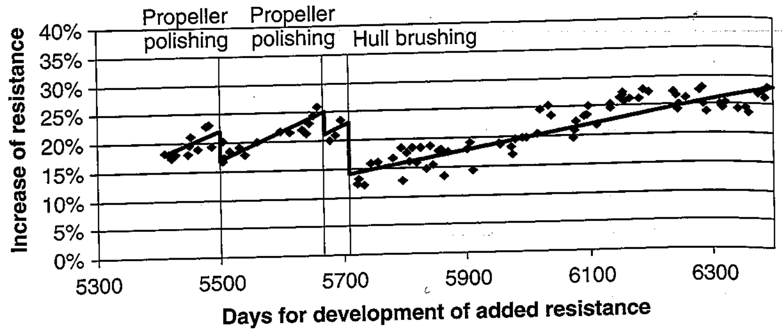

7.12 Added resistance diagram illustrating the decrease in resistance due to two propeller polishings and hull cleaning.

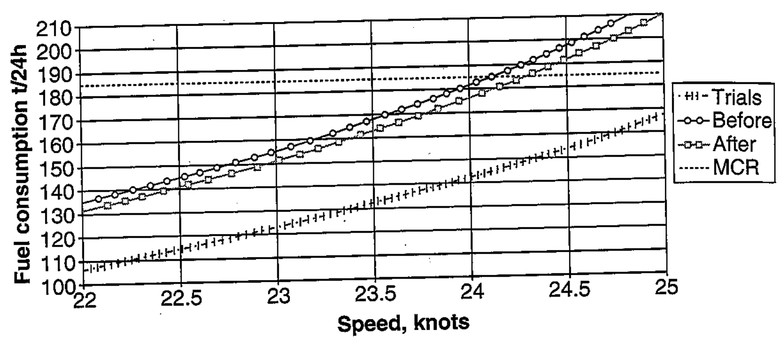

7.13 Fuel consumption versus speed diagram, before and after propeller polishing.

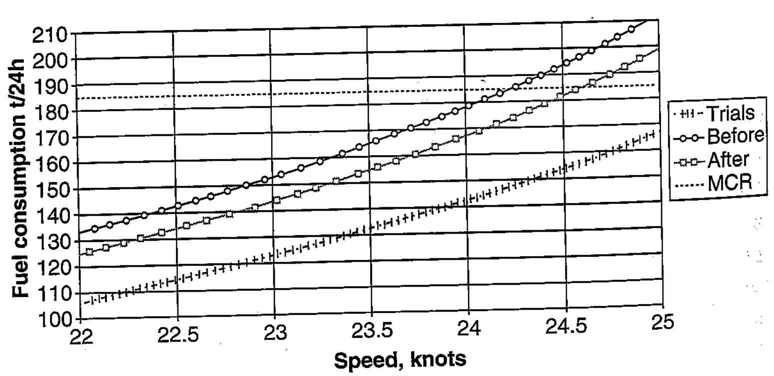

7.14 Fuel consumption versus speed diagram before and after hull brushing.

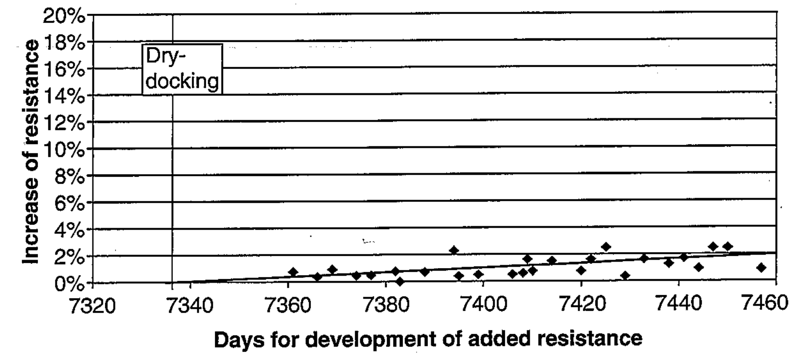

7.15 Added resistance diagram for a 20-year-old dry cargo vessel, illustrating the very low resistance after drydocking attributed to a fully blasted hull pretreatment.

six-month intervals resulted in a fuel savings of five tons per day for each propeller polish, and the hull cleaning resulted in a fuel savings of approximately 12 tons per day. The corresponding speed/power curves for one of the propeller polishings and the hull cleaning are shown in Figs 7.12–7.14. The overall development of resistance of the hull and propeller is 0.7–1% per month. Note that the slope of the line following the hull cleaning is stable and of a similar magnitude as before the hull cleaning, indicating that the hull cleaning was done in time so that a light cleaning removed fouling but did not alter the integrity of the hull coating system. Propeller polishing is a basic, low-cost strategy that saves fuel (Grigson, 1983; NEAA, 2007).

7.9.3 Bulkers

This 20-year-old bulker (see Fig. 7.15) had a very thorough treatment in the drydock, prior to application of a new hull coating system, including straightening of warped hull plates along with a full blast down to bare metal. The results of this drydock treatment are phenomenal, as the added resistance at outdocking was the same as the trial trip. In addition, the resistance is developing quite slowly, with only a 2% increase in resistance appearing after 120 days.

7.10 Benchmarking hull pretreatment in drydock and hull coating systems performance

In the following, four more in-depth examples of the use of the diagrams will be shown as an important tool in vessel performance analysis.

7.10.1 Hull cleanings and drydocking with spot blast

This vessel (see Fig. 7.16) initially had a high added resistance of approximately 50%. When the situation was discovered, the propeller was polished and the ship's sides were brushed. It is seen that the effect of this treatment was marginal. The operator was advised to have the ship drydocked, but as drydocking was inconvenient at that time he decided to clean the sides and bottom of the hull thoroughly a few weeks later. The result of this cleaning was remarkable, but as the antifouling was apparently depleted, the result did not last long (as indicated by the steep slope of the line), and the ship was drydocked on schedule. Subsequent to the drydocking, the hull was cleaned in-water when the added resistance exceeded 20%.

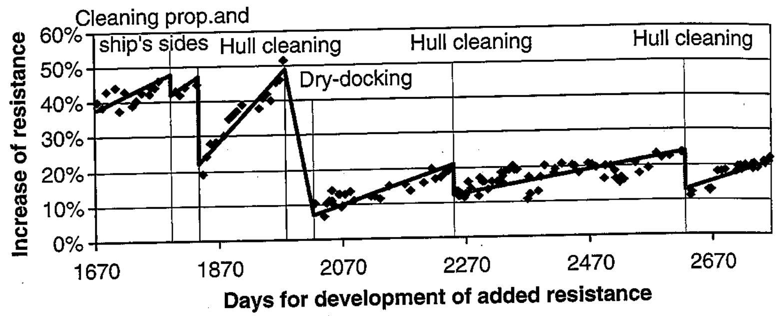

7.16 Added resistance diagram illustrating the changes in resistance due to hull cleanings, drydocking, propeller cleaning, and changes in development due to fouling.

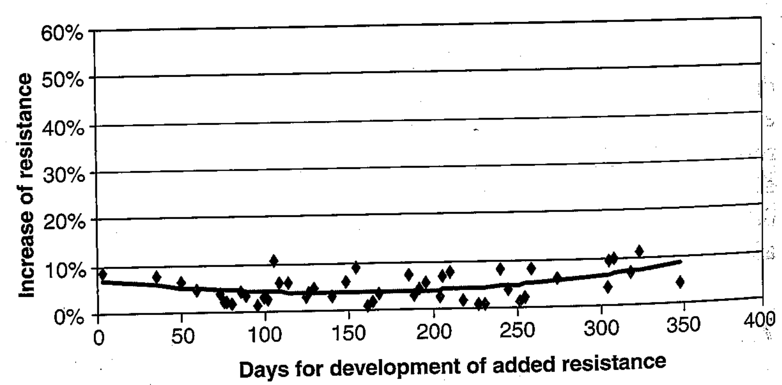

7.17 Added resistance diagram for initial port stay with decreasing resistance due to fouling removal and slow increase in resistance due to fouling.

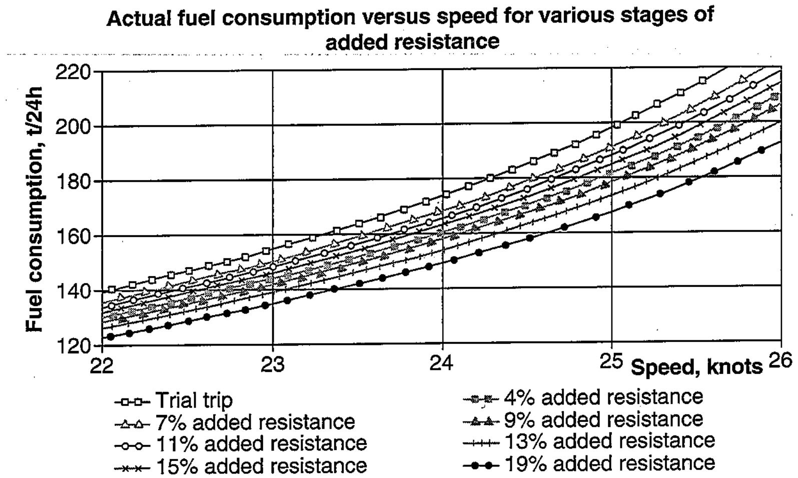

7.18 Fuel consumption versus speed for a fleet of seven similar vessels with the only difference being the added resistance, compared to trial trip vessel performance.

7.10.2 Long port stays

This tanker (see Fig. 7.17) sat for one month prior to its maiden voyage, and it is clear that the vessel accumulated fouling while sitting in port. Upon sailing, the self-polishing copolymer coating was activated, and the fouling and corresponding resistance reduced over the course of one year. The resistance is now developing along normal lines.

7.11 Added resistance as a metric to compare hull and propeller condition of similar vessels

7.11.1 Fleet monitoring

The graph (see Fig. 7.18) shows a fleet of seven vessels of similar design, plotting the actual performance due to their present state of corrosion and fouling, with all other variables corrected. This graph illustrates that performance losses due to fouling are seen as an increase in consumption to maintain a speed or as an incremental speed loss at a maintained power (with no change in fuel consumption; Delft, 2006). Note that in this speed window, the fleet of seven ships varies in fuel consumption from 156 tons per day to 174 tons per day (at 24 knots) due solely to fouling and type of treatment in drydock. Alternatively, the 'speed loss' due to fouling can be measured as a speed loss percentage of the total distance traveled. Significant differences in vessel performance can be attributed to hull and propeller fouling due to different hull coating formulations in connection with vessel age and operational patterns (such as vessel speed, time in port, geographic region of operation, and drydocking time interval; Prochaska, 1981; Townsin and Wynne, 1976).

Please keep in mind that the added resistance percentage is not always equal to the percentage increase in fuel use or the percentage speed loss.

7.11.2 Lessons learned

Analysis over the past ten years on vessels in service has provided some general conclusions that are noteworthy.

1. The added resistance (due to fouling of the hull and propeller) varies from around 6% to 80% in the worst cases. On average, the added resistance for a single displacement hull oceangoing vessel is approximately 30%, if no special attention has been paid to the vessel. A 30% added resistance on an Aframax tanker equates a speed penalty of 1.0 knots – or an increase in fuel use of 12 tons per day at design speed. Thirty per cent added resistance on a high-speed containership equates to a speed loss of 1.8 knots or an increase in fuel use of 70 tons per day at a design speed of 25 knots @ 195 tons per day.
   a) Roughly one-third of all vessels are in good condition with added resistance less than 20%.
   b) Half of all vessels are in reasonable condition, but in a condition that could easily be improved, showing an added resistance of between 20% and 40% but exhibiting no unusual fouling pattern. For these vessels, improvement in performance can be achieved by some standard maintenance procedures without interfering with the normal course of operations.
   c) The remainder of the world fleet (over 10 000 dwt) is in poor condition, showing an added resistance of over 50% (with a good likelihood of biorisk from high levels of hull fouling).
2. The development of added resistance normally follows a curve. The increase will normally be between 0.5% and 2% per month at the beginning of a drydocking period. In some cases, increases of 5%–6% per month for a limited duration have been seen. Later in the period, when the added resistance has reached a certain level, its development may be more restricted. The slope of the lines for development of resistance are a good business tool in determining future performance penalties due to fouling.
3. The basic hull treatment in drydock has a pronounced influence on added resistance after drydocking. In the best cases, the baseline added resistance will only be 0%–4%. A partial hull blasting treatment with new coating system has been seen to result in an added resistance of 5%–20%, while in the worst cases there is no benefit at all from drydocking.
4. The type of hull coating has a pronounced influence on the development of added resistance. It is also important that the coating be applied to the correct thickness, and that the dissolution speed – or, for self-polishing paint, the polishing speed – be carefully adjusted to the service speed and operational patterns of the vessel. As regards the performance of silicon coatings (see Chapter 26), the treatment in drydock is even more critical than with paint systems.
5. Hull cleaning between drydockings may have a remarkable effect, especially if one of the less active types of antifoulants has been used. Hull cleaning may to a certain degree compensate for an antifoulant's low efficiency.

It is advisable to clean the hull *before* the slimy layer of bacteria and algae has turned into a layer of seaweed. In that case, very soft brushes (for example, softer than the bristles of a toothbrush) can be used, and the antifouling system will not be damaged. This stage corresponds to approximately 12% of resistance added to the resistance after drydocking. At a later stage, harder brushes are required, and though they can easily remove seaweed, they will most probably remove some of the antifoulant as well; this removal may result in an increased development of added resistance after the cleaning. The slime associated with foul-release systems has been shown to remain on ship hulls even at 30 knots (Candries *et al.*, 2001)

7.12 Conclusions

Economically optimal precautions can only be taken if the propulsion condition of the vessel is well defined, which requires not only a reliable performance monitoring system, but also rigorous methods of analysis. Any vessel owner/operator may establish such a system; however, significant hydrodynamic and statistical expertise are required in order to develop and extract actionable information for prudent business decisions:

- To evaluate drydocking treatment such as water-blasting, robotic systems, and other emerging technologies.
- To follow the development of hull and propeller resistance for individual vessels and to take action, when economically justified, on a vessel-to-vessel basis. Such action includes evaluating the before-and-after effect of hull cleanings, by divers with brushing machines, underwater robotic hull cleaning and propeller polishing, as well as the mitigation of invasive species introduced through the vessel hull.

- To benchmark the efficiency (total ownership cost) of any coating system by comparing vessels with different coating systems; vessels need not be identical in hull form.

Experience has shown that at least 10% may be saved on average on fuel costs for lightly fouled hulls, and up to 35% may be saved when hulls are heavily fouled. For a ship that burns 100 tons of fuel per day, such as a very large crude carrier or medium-size containership, at least 10 tons per day may be saved, corresponding to 31.9 tons of CO_2 emissions reduction. With bunker fuel prices at 300 USD per ton, that represents a value of approximately 3000 USD per day. Some naval vessels exhibit a 15% decrease in fuel consumption attributable to hull and propeller cleanings (US Navy and EPA, 2003).

7.13 Sources of further information and advice

Ship trials with biocide-free antifouling paints in Australian waters (12:15–12:45) **J. Lewis** (Defence Science & Technology Organisation, Melbourne) http://www.limnomar.de/download/05-Workshop-A-Lewis.pdf

Outcome of the research project 'Performance of biocide-free antifouling paints for deep-sea going vessels' (11:45–12:15) **B. Daehne** (LimnoMar) http://www.limnomar.de/download/04-Workshop-A-Daehne.pdf

The Development of Foul Release Coatings for Ocean Going Vessels http://www.imarest.org/proceedings/samples/candries_coatings.pdf

7.14 References

Anderson C, Atlar M, Callow M, Candries M and Townsin R L (2003), 'The development of foul-release coatings for seagoing vessels', proceedings of the Institute of Marine Engineering, Science and Technology, Part B, *Journal of Marine Design and Operations*, 4, 11–23.

Anon (2008). Hempasil: Fuel Savings. http://www.hempel.com/.

Bohlander G S (1991), 'Biofilm effect on drag: measurements on ships,' Paper 16. In: *Polymers in a Marine Environment*; Marine Management (Holdings), October 1991, pp. 1–4.

Buhaug Ø (2005), 'Assessment of CO_2 emission performance of individual ships: the IMO CO_2 index', *Marintek*.

Candries, M and Atlar, M (2005), 'Experimental investigation of the turbulent boundary layer of surfaces coated with marine antifoulings', *Journal of Fluids Engineering*, 127 (2), 219–232.

Candries M, Atlar C D and Anderson C (2001), '*Foul release systems and drag*', Newcastle-upon-Tyne: University of Newcastle-upon-Tyne.

Candries M, Atlar M, Mesbahi E and Pazouki K (2003), 'The measurement of the drag characteristics of tin-free self-polishing co-polymers and fouling release coatings using a rotor apparatus', *Biofouling*, 19 (supplement), 27–36.

Conn J F C, Lackenby H and Walker W P (1953), 'Resistance experiments on the Lucy Ashton,' *Trans INA* 95, 350–436.

Delft C E (2006), 'Greenhouse gas emissions for shipping and implementation guidance for the marine fuel sulphur directive', *IMO Report*, 2006 (Dec).

Grigson C W B (1983), '*Propeller roughness, its nature, and its effects upon the drag coefficients of blades and ship power*', London: Royal Institute of Naval Architects.

Haslbeck E (2003), '*ASTM methods for efficacy testing of biocide-free antifouling paints*,' US Navy.

Holm E, Schultz M, Haslbeck E, Talbott W and Field A (2004), 'Evaluation of hydrodynamic drag on experimental fouling-release surfaces, using rotating disks', *Biofouling*, 20 (4–5), 219–226.

IMO (2000), 'Study of GHG emissions from ships', *Marintek* (Mar).

Kempf G (1937), 'On the effects of roughness on the resistance of ships,' *Trans INA* 79, 109–119.

Lewkowicz A and Das D K (1986), 'Turbulent boundary layers on rough surfaces with and without a pliable overlay: a simulation of marine fouling,' *Int. Shipbuilding Prog.*: 174–185.

Lewthwaite J C, Molland A F and Thomas K W (1985), 'An investigation into the variation of ship skin frictional resistance with fouling,' *Trans RINA* 127, 268–279.

Loeb G, Laster D and Gracik T (1984), 'The influence of microbial fouling films on hydrodynamic drag of rotating disks,' In: Costlow, JD, Tipper, RC (eds) *Marine biodeterioration: an interdisciplinary study*. US Naval Institute Press, Annapolis, MD, USA, pp. 88–94.

Man B & W (2004), '*Basics of Ship Propulsion*', April 2004.

Netherlands Environmental Assessment Agency (2007), '*Analysis of options for including international aviation and marine emissions in a post-2012 climate mitigation regime*,' The Hague, Netherlands Environmental Assessment Agency, p. 39.

Prochaska F (1981), '*Timing of drydock intervals to most economic effect*', Jersey City, Society of Naval Architects and Marine Engineers.

Schetz J A (1993), *Boundary Layer Analysis*. Prentice-Hall, EnglewoodCliffs, NJ.

Schultz M P (2004), 'Frictional resistance of antifouling coating systems', *Journal of Fluids Engineering*, 126, 1039–1047.

Schultz M P (2007), 'Effects of coating roughness and biofouling on ship resistance and powering', *Biofouling*, 23 (5), 331–341.

Schultz M P and Flack K A (2007), 'The rough-wall turbulent boundary layer from the hydrodynamically smooth to the fully rough regime', *Journal of Fluid Mechanics*, 580, 381–405.

Schultz M P and Swain G W (1999), 'The effect of biofilms on turbulent boundary layers', *Journal of Fluids Engineering*, 121 (1), 44–45.

Schultz M P and Swain G W (2000), 'The influence of biofilms on skin friction drag', *Biofouling* 15, 129–139.

Swain G (2007), '*Measuring the performance of today's antifouling coatings*', Florida Institute of Technology.

Swedish Network for Transport and the Environment, *Comparitive Carbon Dioxide Emissions*.

Townsin R L (2003), 'The ship hull fouling penalty', *Biofouling* 19 (Supplement 1) 9–15.

Townsin R and Wynne J L (1976), '*Hull condition, penalties and palliatives for poor performance*', Newscastle: University of Newcastle.

US Navy and EPA (2003), '*Feasibility impact analysis report underwater ship husbandry*'.

Watanabe S, Nagamatsu N, Yokoo K and Kawakami Y (1969), 'The augmentation of frictional resistance due to slime', *J. Kansai. Soc. Nav. Arch.* 31, 45–51 (in Japanese) BSRA translation 3454.

Weinell C E, Olsen K N, Christoffersen M W and Kiil S (2003), 'Experimental study of drag resistance using a laboratory scale rotary set-up', *Biofouling*, 19 (supplement), 45–51.